Side-chain Charge Effects and Conductance Determinants in the Pore of ClC-0 Chloride Channels

Mei-Fang Chen and Tsung-Yu Chen

Center for Neuroscience and Department of Neurology, University of California, Davis, CA 95616

ABSTRACT The charge on the side chain of the internal pore residue lysine 519 (K519) of the *Torpedo* ClC-0 chloride (Cl^-) channel affects channel conductance. Experiments that replace wild-type (WT) lysine with neutral or negatively charged residues or that modify the K519C mutant with various methane thiosulfonate (MTS) reagents show that the conductance of the channel decreases when the charge at position 519 is made more negative. This charge effect on the channel conductance diminishes in the presence of a high intracellular Cl^- concentration ($[Cl^-]_i$). However, the application of high concentrations of nonpermeant ions, such as glutamate or sulfate (SO_4^{2-}), does not change the conductance, suggesting that the electrostatic effects created by the charge at position 519 are unlikely due to a surface charge mechanism. Another pore residue, glutamate 127 (E127), plays an even more critical role in controlling channel conductance. This negatively charged residue, based on the structures of the homologous bacterial ClC channels, lies 4–5 Å from K519. Altering the charge of this residue can influence the apparent Cl^- affinity as well as the saturated pore conductance in the conductance-Cl^- activity curve. Amino acid residues at the selectivity filter also control the pore conductance but mutating these residues mainly affects the maximal pore conductance. These results suggest at least two different conductance determinants in the pore of ClC-0, consistent with the most recent crystal structure of the bacterial ClC channel solved to 2.5 Å, in which multiple Cl^--binding sites were identified in the pore. Thus, we suggest that the occupancy of the internal Cl^--binding site is directly controlled by the charged residues located at the inner pore mouth. On the other hand, the Cl^--binding site at the selectivity filter controls the exit rate of Cl^- and therefore determines the maximal channel conductance.

KEY WORDS: ClC-0 • electrostatic effect • surface charge • pore conductance

INTRODUCTION

ClC channels conduct chloride (Cl^-) ions across membranes of various cells, and thus play important roles in various physiological processes such as maintenance of membrane potential, control of intracellular pH, and perhaps regulation of cell volume (Jentsch et al., 1999, 2002; Maduke et al., 2000; Iyer et al., 2002). ClC-0, which is present in the *Torpedo* electric organ, is the first cloned member of this channel family (Jentsch et al., 1990; O'Neill et al., 1991). In comparison with the other ClC channels, this *Torpedo* Cl^- channel is relatively well characterized in its functional behaviors (for reviews of the molecular operations of ClC-0 see Miller and Richard, 1990; Maduke et al., 2000). Previous studies have revealed an interesting property related to the ion permeation in the ClC-0 pore: the channel's conductance is regulated by the side-chain charge of residue 519 (Middleton et al., 1996). When the wild-type (WT)* lysine residue (K519) is replaced with a neutral or a negatively charged residue, the pore conductance is decreased. Because the alteration of the pore conductance concurs more with the charge instead of the size or the shape of the side chain, the regulation was thought to be a through-space electrostatic effect, and thus K519 was suggested to be located within a Debye length from the internal pore entrance of ClC-0 (Middleton et al., 1996).

The location of K519 near or in the pore mouth is supported by the recently solved high-resolution crystal structures of bacterial ClC channels (Dutzler et al., 2002). The structure of the bacterial ClC channels revealed positively charged amino acids that might help funnel Cl^- ions into the pore entryways. These basic residues include R147 and R451, which are located at the proposed extracellular and intracellular pore vestibules of the channel, respectively. From a functional viewpoint, R451 of the bacterial ClC channels would correspond to K519 of ClC-0. However, sequence alignment indicates that R451 and T452 of the bacterial channels correspond to I518 and K519 of ClC-0, respectively (Dutzler et al., 2002). Clarifying this ambiguous sequence alignment is important because the position of a charge in the pore region could be critical for the conductance determinants of an ion channel.

Mei-Fang Chen's present address is Neuro-Medical Scientific Center, Tzu Chi General Hospital, 707, Sec. 3, Chung-Yang Rd., Hualien 970, Taiwan.

Address correspondence to Tsung-Yu Chen, Center for Neuroscience, University of California-Davis, 1544 Newton Court, Davis, CA 95616. Fax: (530) 754-5036; email: tycchen@ucdavis.edu

Abbreviations used in this paper: ACh, acetylcholine; HEK, human embryonic kidney; MTS, methane thiosulfonate; WT, wild-type.

J. Gen. Physiol. © The Rockefeller University Press • 0022-1295/2003/08/133/13 $8.00
Volume 122 August 2003 133–145
http://www.jgp.org/cgi/doi/10.1085/jgp.200308844

Furthermore, since the exact functional roles of charged residues in the pore of ClC channels are still murky, exploring how K519 of ClC-0 controls the pore conductance is imperative. Electrostatic regulation of ion permeation (and thus channel conductance) has been observed in many other channels. Imoto et al. (1986, 1988) suggested that rings of negatively charged amino acids near the pore mouth of the nicotinic acetylcholine (ACh) receptor channel might serve to raise the local cation concentration and thus increase the channel conductance. Later experiments, however, suggested that this effect in the ACh receptor channel was not consistent with a surface charge mechanism (Pappone and Barchfeld, 1990; Kienker et al., 1994). On the other hand, a surface charge effect was demonstrated in the large-conductance Ca^{2+}-activated K^+ channel (MacKinnon and Miller, 1989; MacKinnon et al., 1989). For anion channels, the glycine receptor channel contains positively charged residues in the pore region that may help the permeation of anions across the channel pore (Keramidas et al., 2000). These basic residues in the pore of the glycine receptor channel most likely exert their influence on the ion-binding sites important for Cl^- permeation.

The presence of a charge in the pore, however, creates a paradox for ion permeation. On the one hand, the charge may attract a "cloud" of counter-charged ions to the pore and favor a high conductance. On the other hand, the charge of the side chain may also increase the binding affinity for the counter-charged ion, and thus generate a deep energy well in the ion permeation process that reduces the ion flux through the pore. The most recent crystal structure of the *E. coli* ClC channel at 2.5-Å resolution (Dutzler et al., 2003) reveals three Cl^--binding sites in the presumably "open" pore: one at the previously identified Cl^- selectivity filter (the central site, S_{cen}) (Dutzler et al., 2002), and two other binding sites each respectively located at the external (S_{ext}) and internal (S_{int}) side of S_{cen}. Could the electrostatic force from the K519 side chain affect Cl^- binding to any of these three binding sites, or does the positive charge from K519 merely generate a surface charge effect? We studied these questions by exploring the functional roles of amino acid residues in the inner pore region under the guidance of the bacterial ClC channel structures. The positions where charge alterations were made in the present study included K519, E127, and I515. In addition, effects of mutating two key residues at the Cl^- selectivity filter, S123 and Y512, were also examined. The locations of the corresponding residues in the bacterial ClC channel together with the two Cl^- ions at S_{cen} and S_{int} are shown in Fig. 1. These residues surround the Cl^--binding sites, and therefore are likely to contribute to the conductance determinants in the pore of ClC-0, which a Cl^- ion would encounter in its journey from the internal pore mouth to the ion selectivity filter. The results show that the charge effect from K519 on channel conductance is not consistent with a simple surface charge mechanism. In addition, the negatively charged residue E127, which is located at a position close to K519, plays an even more critical role in controlling the pore conductance of ClC-0. The different mutation effects for residues along the ion permeation pathway are consistent with ClC-0 also having multiple ion-binding sites in the pore, with charged residues at the inner pore mouth controlling the conductance of ClC-0 by affecting the Cl^- occupancy at S_{int}.

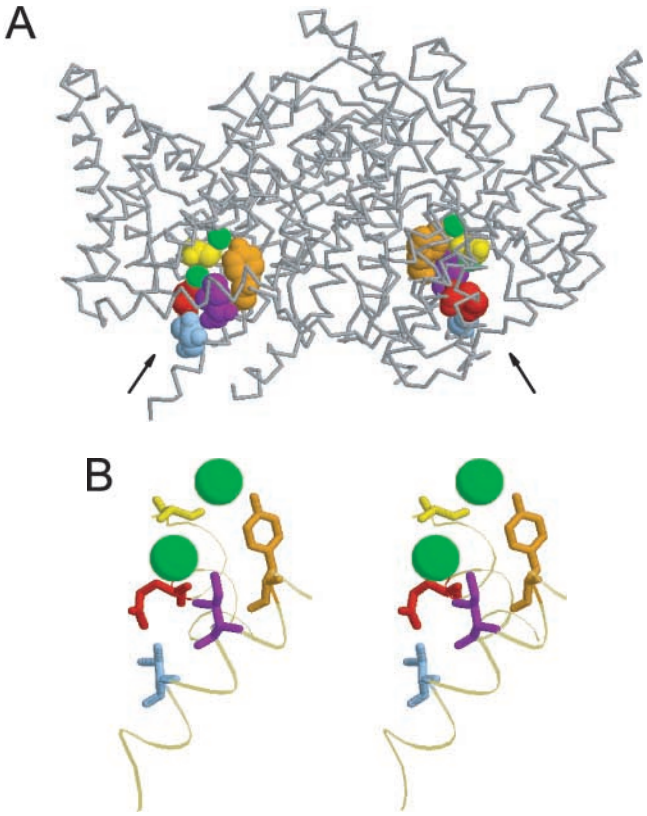

FIGURE 1. Positions of the mutated pore residues of ClC channels. Side views of the *E. coli* ClC channel. Extracellular side is on top. Structural coordinates are taken from Protein Data Bank (code 1OTS) with the cocrystallized antibody molecules removed. (A) Residues of the bacterial ClC channel that correspond to those of ClC-0 examined in the present study. The color codes are (ClC-0 numbers in parentheses): blue, T452 (K519); red, E111 (E127); purple, I448 (I515); yellow, S107 (S123); orange, Y445 (Y512). Cl^- ions at S_{cen} and S_{int} are shown in green. Arrows indicate the intracellular pore entrances. (B) Stereo view of the mutated residues in the pore. Only those residues in the left subunit in A are shown. The residues (same color codes as in A) are represented by sticks to show the relations of their side chains with the two Cl^- ions in the pore. Thin faint ribbons represent helices D and R, on which these residues are located.

MATERIALS AND METHODS

Site-directed Mutagenesis and Channel Expression

The WT *Torpedo* ClC-0 channel and an inactivation-suppressed mutant C212S (Lin et al., 1999) both contain a lysine residue at position 519. The fast-gating and permeation properties of these two channels were not distinguishable (Lin et al., 1999; Pusch et al., 2001), and therefore they were considered together as the WT channel containing a positive charge at the position 519. Various mutants at position 519 were a gift from Dr. Chris Miller. The mutations were initially constructed in the pcDNA3 vector (Invitrogen) with several silent mutations incorporated in the sequence of the original WT cDNA to create unique restriction enzyme cutting sites. The WT channels expressed from this "synthetic" plasmid in HEK293 cells (Middleton et al., 1996) or in *Xenopus* oocytes (unpublished data) show the same properties as those of the genuine WT channels. Various mutations at the position 519 that were studied include K519R, K519C, K519H, K519M, K519E, and K519D. The other mutants include the mutations of E127, I515, I518, S123, and Y512. The cDNAs of these mutants were all constructed in the pBluescript vector (Stratagene). To make RNA, the plasmids were linearized by restriction enzyme ScaI (New England Biolabs, Inc.). Capped RNAs were synthesized with T3 polymerase using a mMessage mMachine kit (Ambion). *Xenopus* oocytes were prepared and injected with RNAs as described previously (Chen, 1998).

Electrophysiological Recordings, Solution Exchange, and MTS Modifications

Whole oocyte recordings using standard two-electrode voltage clamp techniques similar to those described before (Chen, 1998; Lin et al., 1999; Chen and Chen, 2001) were performed to estimate the expression level of the channels suitable for single-channel studies. The single-channel recordings were performed using excised inside-out patch configurations (Hamill et al., 1981). The recording pipettes were pulled from borosillicate glass capillaries (World Precision Instruments) using PP-830 puller (Narashige), and when filled with the external solution, had resistance of 3–6 MΩ. In all experiments, the pipette (external) solution contained (in mM): 110 NMDG-Cl, 5 $MgCl_2$, 1 $CaCl_2$, 5 HEPES, pH 7.5. The standard bath (internal) solution in which a high GΩ seal was achieved contained (in mM): 110 NaCl, 5 $MgCl_2$, 1 EGTA, 5 HEPES, pH 7.5. The pHs of the internal and external solutions were titrated with NaOH and NMDG, respectively. In most recordings, the current was filtered at 200 Hz (3dB, 4 pole Bessel) and was digitized by an acquisition board (model DAP 820; Microstar Laboratories, Inc.) at 1 kHz with homemade software (Chen and Miller, 1996; Lin et al., 1999; Lin and Chen, 2000; Chen and Chen, 2001). For I515K mutant, the gating of the channel is fast. Therefore, we filtered and digitized the current at 0.5 and 2.5 kHz, respectively.

The solution exchange was achieved using SF-77 solution exchange system (Warner Instruments, Inc.). After obtaining the excised inside-out patch configuration, the patch was brought very close to the outflow of solution perfusion pipes. The motor of the SF-77 solution exchange system was controlled by an analogue signal delivered from the DAP board, and the solution exchange was usually completed within ~20–50 ms. Except where indicated, the various internal solutions contained (in mM): (X-10) NaCl, 5 $MgCl_2$, 1 EGTA, 5 HEPES, pH 7.5, where X represents the indicated $[Cl^-]_i$. To make solutions with a Cl^- concentration less than 120 mM (such as 30 or 60 mM), Na-glutamate was added to make the ionic strength similar to the 120 mM Cl^- solution.

Modification of the introduced cysteine was performed with MTS reagents purchased from Toronto Research Chemicals. Stock solutions of 0.1 M were prepared in water and stored at −80°C. Working solutions containing 30–300 μM of the MTS reagents were made immediately before use. The modification of the cysteine in the K519C mutant was usually completed within 30 s after the exposure of the patch to the solutions containing MTS reagents.

Data Analysis

Analysis of the single-channel recording trace was performed using a home-written program (Chen and Miller, 1996; Lin et al., 1999; Lin and Chen, 2000; Chen and Chen, 2001). Because single-channel conductance for some mutant channels are small (for example, K519C and K519E), all the single-channel traces were further subjected to digital filtering, leading to a final filter frequency of ~140 Hz. Even at this filtering frequency, the signal-to-noise ratio was still not high enough to reliably resolve open-close transitions of the K519E mutant at symmetrical 120 mM $[Cl^-]_i$. Therefore, the recording of the K519E mutant at $[Cl^-]_i$ = 120 mM was not analyzed.

Single-channel current amplitudes were determined from all-points amplitude histograms, which show three distinct peaks due to the "double-barrel" nature of the channel (Miller, 1982; Miller and White, 1984; Bauer et al., 1991; Middleton et al., 1994, 1996; Ludewig et al., 1996; Lin and Chen, 2000; Pusch et al., 2001). The conductance of the channel is estimated by fitting the data points between −50 and −110 mV in the single-channel i-V plot to a straight line. To examine the internal Cl^- effect on the conductance and the gating parameters more closely, we converted $[Cl^-]$ into Cl^- activity ($A_{Cl-} = \mu[Cl^-]$), using the following activity coefficients (μ): 30 mM, 0.930; 60 mM, 0.867; 120 mM, 0.769; 300 mM, 0.710; 600 mM, 0.673; 1,200 mM, 0.654; 2,400 mM, 0.684 (Robinson and Stokes, 1955).

All results are presented as mean ± SEM. Curve fitting was performed with an unweighted, least-squares method using Origin software (OriginLab Co.).

RESULTS

Effects of Charges from Positions 518 and 519 on the Pore Conductance

The regulation of the channel conductance of ClC-0 by the charge at position 519 was first shown in bilayer recordings of the purified *Torpedo* ClC-0 channels expressed in human embryonic kidney (HEK) 293 cells (Middleton et al., 1996). This side-chain charge effect can be reproduced using various manipulations on the channel expressed in *Xenopus* oocytes. One approach to alter the charge of residue 519 is via site-directed mutagenesis (Fig. 2 A). Under the same recording condition, the WT channel (with lysine at position 519, K519) has the largest single-channel current, followed by K519C, a replacement by a neutral residue, and then by K519E, a mutant with a negative charge at position 519. Alternatively, the electrostatic effect can be achieved by chemical modifications of the K519C mutant with various MTS reagents (Fig. 2 B). When the cysteine at position 519 is modified with 2-aminoethyl MTS (MTSEA) or 3-aminopropryl MTS (MTSPA), the

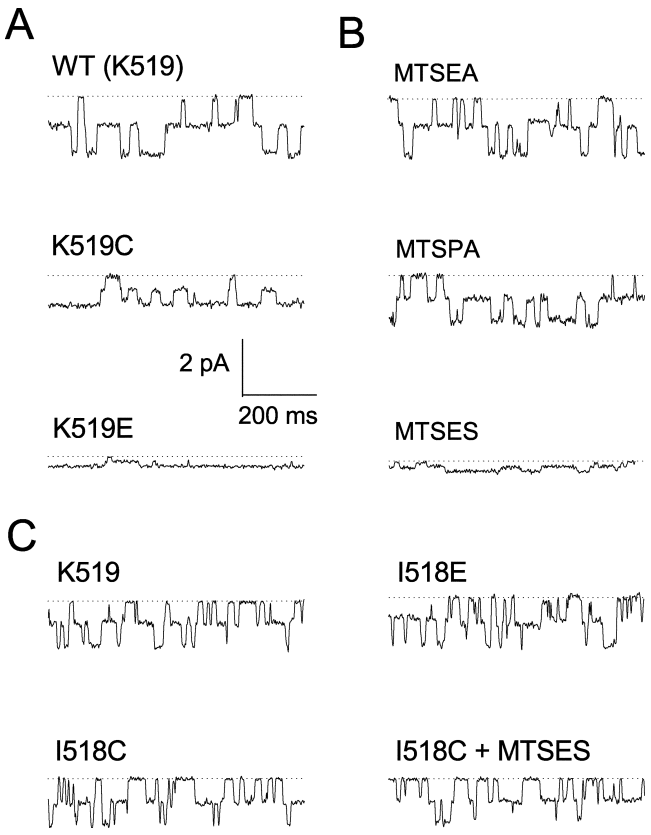

FIGURE 2. The charge from position 519 exerts more influence on the conductance of ClC-0 than that from position 518. All recording traces are from excised inside-out patches. (A) Recordings of WT (K519), K519C, and K519E mutants. In all experiments, $[Cl^-]_o$ = 120 mM, $[Cl^-]_i$ = 300 mM, and V_m = −80 mV. (B) Single-channel recordings of the K519C mutant after the introduced cysteine is modified with MTSEA, MTSPA, and MTSES. Same recording conditions as in A. (C) Effect of the charge placed at position 518 on the channel conductance. Single-channel recordings were made at −90 mV. $[Cl^-]_o$ = 120 mM and $[Cl^-]_i$ = 120 mM. For the recording of the MTSES-modified I518C, the trace was taken 110 s after the application of 300 μM MTSES to the patch. Scale bars in A apply to B.

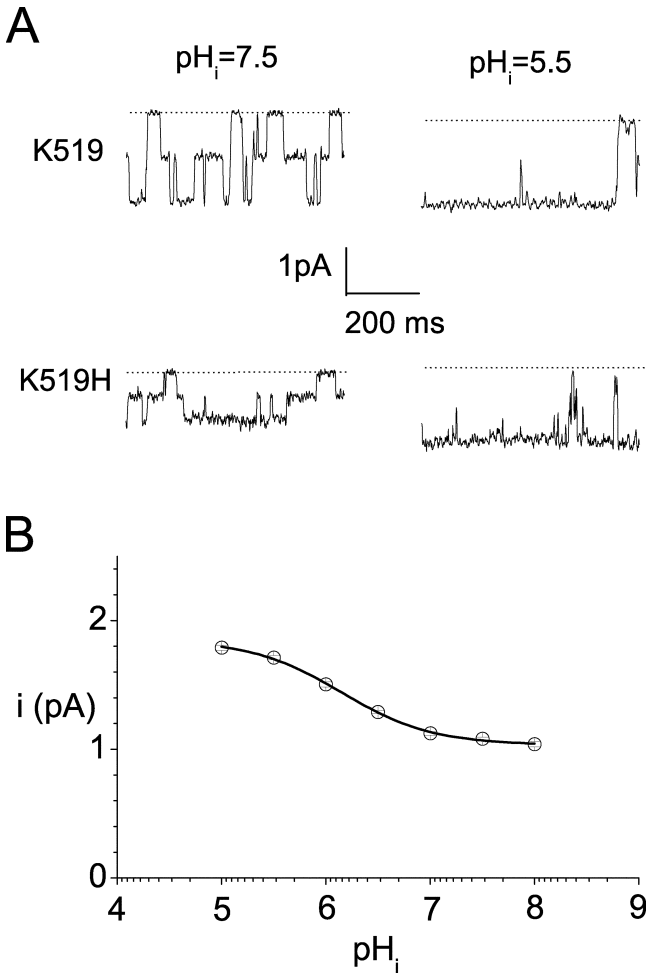

FIGURE 3. Effect of intracellular pH on the single-channel conductance of the WT (K519) or K519H channel. (A) Single-channel recording traces of K519 and K519H channels at two different pH_i. Dotted lines are the zero-current level. The ionic conditions are as in Fig. 2 A. V_m = −70 mV. (B) Titration of the single-channel current of the K519H channel by pH_i. Experimental conditions are as described in A. The current values were determined between the zero-current level and the fully open level in the amplitude histogram (because of the sparsity of the middle current level at low pH_i), therefore reflecting the sum of the current of two pores. Solid curve is drawn according to a logistic function, $A_1 + (A_2 - A_1)/(1 + [H^+]_o/K_a)$, where K_a is the dissociation constant of protonation. The minimal (A_1) and maximal (A_2) current were 1.02 and 1.82 pA, respectively. The fitted pK_a is 6.18.

side-chain of K519C is attached with a positive charge, and the single-channel current is similar to that of the WT channel. On the other hand, after the cysteine is modified with 2-sulfonatoethyl MTS (MTSES), which attaches a negatively charged group on the cysteine side chain, the current amplitude is similar to that of the K519E mutant. These results are all consistent with those shown in Middleton et al. (1996).

Comparison of the sequences indicates that R451 of StClC corresponds to I518, while T452 of StClC aligns with K519 of ClC-0 (Dutzler et al., 2002). To investigate the possibility that a charge at position 518 in ClC-0 may have a similar electrostatic contribution on the channel conductance, we mutate I518 of ClC-0 into cysteine and glutamate. Fig. 2 C shows the single-channel recording traces of I518C, I518E, and the MTSES-modified I518C. In comparison with the conductance changes in the K519 mutants (Fig. 2, A and B), the electrostatic influence from a negative charge placed at position 518 is negligible. The crystal structure of bacterial ClC channels reveals that the side chain of T452, but not that of R451, is located deeper in the ion conduction pathway (Dutzler et al., 2002, 2003). Thus, a charge at position 519 should exert more electrostatic influence on the pore conductance than at position

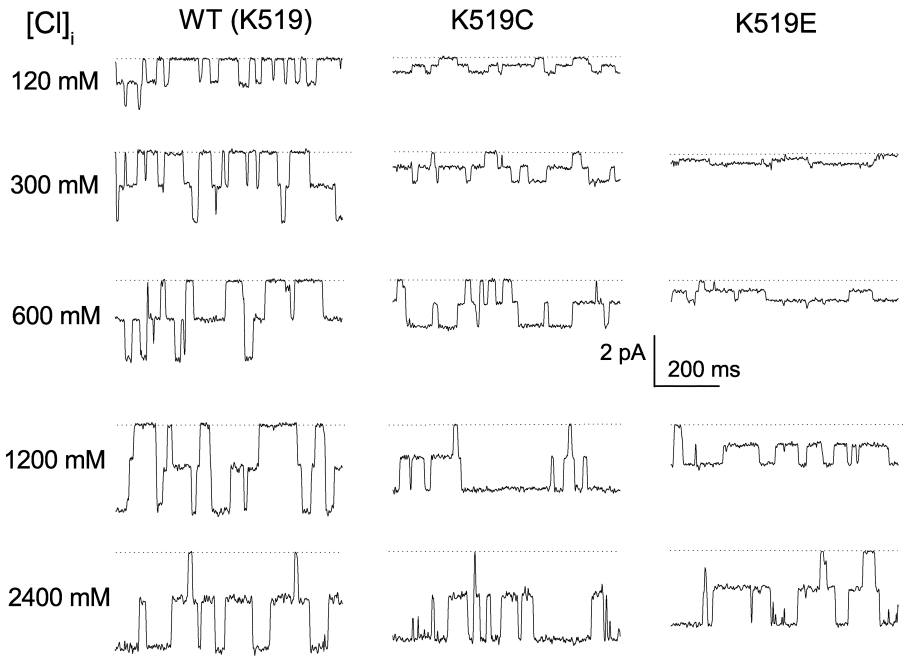

FIGURE 4. Single-channel recordings of ClC-0 channels with various charges at position 519 in different $[Cl^-]_i$. For all recordings, the pipette (extracellular) solution contains 120 mM Cl^-. $[Cl^-]_i$ is varied as indicated. $V_m = -110$ mV. Dotted lines represent zero-current level.

518. We therefore suggest that K519 of ClC-0 corresponds to T452, but not R451 of bacterial ClC channels.

The change in the conductance of ClC-0 affected by replacing K519 with various amino acids is mostly due to the charge rather than the size or shape of the side chain of the amino acids. Therefore, mutants such as K519C, K519Q, K519M, and K519F all have a similar channel conductance, while the conductance of K519R is close to that of the WT (K519) channel (unpublished data; also see Middleton et al., 1996). To demonstrate a pure charge effect on the channel conductance, we examined a channel in which K519 was replaced by histidine (K519H). The side-chain of histidine carries a positive charge at low pH but is neutral at a higher pH. The conductance of K519H mutant should vary according to the intracellular pH (pH_i). Fig. 3 A compares the recording traces of the K519 (WT) and the K519H channels at two pH_i conditions. Although the fast-gating behavior of the K519 channel is altered by pH_i (also see Hanke and Miller, 1983), the channel conductance remains the same when pH_i is switched between 7.5 and 5.5. For the K519H mutant, however, the conductance is smaller at $pH_i = 7.5$ (6.2 ± 0.1 pS, $n = 9$) than at $pH_i = 5.5$ (9.8 ± 0.1 pS, $n = 3$). Fig. 3 B plots the single-channel current of the K519H mutant as a function of pH_i, and curve fitting shows that the minimal current is ~56% of the maximal current. In these experiments, the only structural difference on the side chain of residue 519 between two different pH_i conditions is a proton. Thus, these results are consistent with the conclusion that residue 519 influences Cl^- permeation primarily by an electrostatic mechanism.

Side-chain Charge Effect Is Less Prominent at High Cl^- Concentrations

One potential mechanism of the charge effect on the channel conductance is a simple surface charge mechanism—that is, the charge increases the conductance by raising the local concentration of permeant ions in the mouth of the pore (Green and Andersen, 1991). To be consistent with such a surface-charge mechanism, however, two phenomena must be fulfilled. First, the effect of the charge on the conductance is more pronounced at low concentrations of permeant ions and is attenuated at high permeant ion concentrations. Second, the charge effect should be screened in a high ionic strength condition, for example, in the presence of high concentrations of nonpermeant ions (Green and Andersen, 1991; Hille, 2001). To examine these two criteria, we first recorded WT and mutant channels at various internal Cl^- concentrations ($[Cl^-]_i$). Fig. 4 shows representative current traces for the K519, K519C, and K519E channels recorded at −110 mV. For all three channels, the single-channel current is increased with $[Cl^-]_i$, but the concentration ranges in which the current amplitude steeply rises are different among these channels. For the K519 channel, the increase occurs mostly at 120–600 mM; for K519C and K519E mutants, it occurs at all concentrations of $[Cl^-]_i$. Even between 1,200 and 2,400 mM, there is still a large increase in the single-channel current in these two mutant channels.

The recordings of these three channels at various $[Cl^-]_i$ were also examined at different voltages. The averaged single-channel i-V curves are shown in Fig. 5 A. When only the inward current (outward Cl^- movement) is considered, the i-V curves are quite linear for

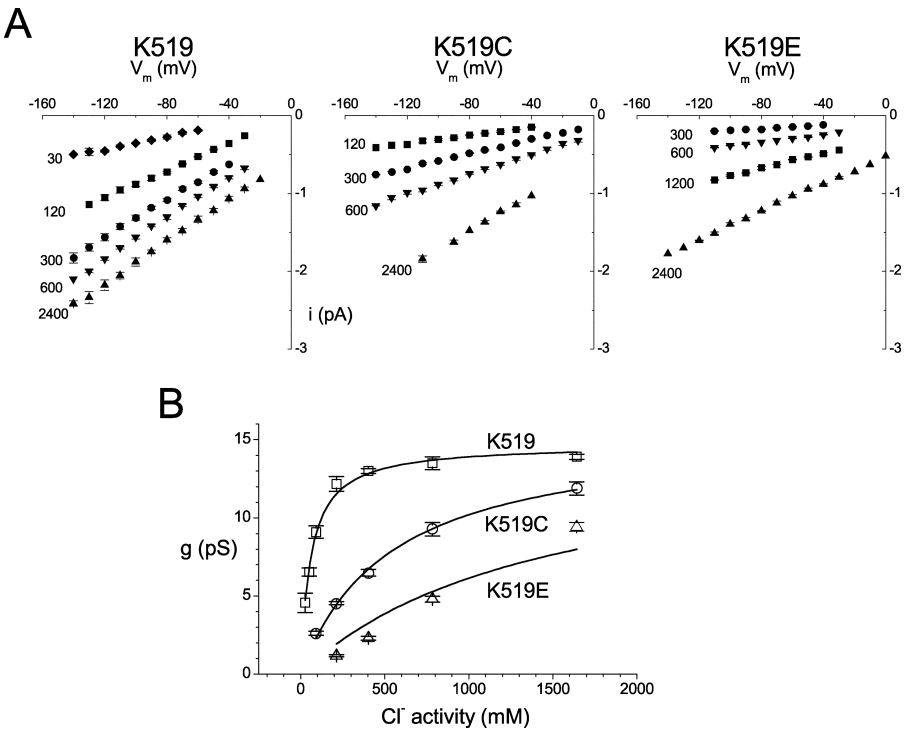

FIGURE 5. Dependence of ClC-0 conductance on internal Cl^-. (A) Single-channel i-V curves of the WT, K519C, and K519E channels at various $[Cl^-]_i$. Data points were derived from experiments like those in Fig. 4. All current amplitudes were measured from single pores. Numbers in the plots are the internal Cl^- concentrations. (B) Single-channel conductance of the WT and the mutant channels as a function of intracellular Cl^- activity. Symbols are: squares, WT (K519); circles, K519C; triangles, K519E. Solid curves are fitted to a Michaelis-Menten equation (Eq. 1b). See Table I for the values of the fitted parameters, g_{max} and $K_{1/2}$.

all three channels, but the slopes of the curves for K519C and K519E mutants are significantly smaller than those of the WT K519 channel at any given $[Cl^-]_i$ (Fig. 5 A). To estimate the single-channel conductance, we fit the data points from −50 to −110 mV to a straight line. Fig. 5 B plots the conductance of these channels as a function of internal Cl^- activity. In the K519 channel, the slope conductance of the channel saturates to a value of ~14.7 pS, and the half-saturating Cl^- activity is ~59 mM. In K519C, the maximum conductance for this mutant is similar to that of the K519 channel: ~15.7 pS. However, the Cl^- activity at the half-maximal conductance is significantly increased to ~534 mM. For the K519E mutant, the four data points are not reasonably well fitted to a single Michaelis-Menten type equation. However, it is apparent that the conductance recorded at the highest concentration (2,400 mM) approaches the maximal conductance of the K519 and K519C channels. To estimate the half-saturating Cl^- concentration, we force the maximal conductance of the K519E mutant to be 15 pS, and the fitted half-saturating Cl^- activity is ~1,444 mM.

Nonpermeant Anions Cannot Screen Out the Electrostatic Effect on the Pore Conductance

The above results thus appear to be consistent with the first criterion of the general surface charge mechanism because the channels with a positive, neutral, or negative charge at position 519 all have a similar saturated conductance. To test the second criterion, we apply high concentrations of large anions such as glutamate and sulfate (SO_4^{2-}). The recording traces of the WT channel (in 120 mM $[Cl^-]_i$) in the absence or in the presence of additional SO_4^{2-} ions are compared in Fig. 6 A. Averaged data in Fig. 6 B show that up to 480 mM of SO_4^{2-} is unable to reduce the current carried by 120 mM Cl^- at any voltage. Similar experiments were also performed at 60 mM $[Cl^-]_i$, and no charge screening effect is observed (Fig. 6 C). There was also no charge screening when up to 480-mM glutamate was present in the solution (unpublished data). These results thus rule out the supposition that a general surface charge mechanism is responsible for the observed electrostatic influence from K519 on the channel conductance.

Functional Role of a Negatively Charged Residue E127 in Controlling the Pore Conductance

What then is the mechanism underlying the side-chain charge regulation on the pore conductance? One possibility is that this electrostatic effect could be due to an effect on the occupancy of the Cl^--binding site in the pore. Crystal structures of the bacterial ClC channels show that T452 of StClC is not immediately adjacent to the Cl^--binding sites S_{cen} and S_{int}. The distances from the α carbon of T452 to the Cl^- ions at S_{cen} and S_{int} are ~15 or ~9 Å, respectively (Fig. 1). On the other hand, a negatively charged residue, E111 (corresponding to E127 of ClC-0), appears to be closer to these two binding sites than the residue T452 (Fig. 1). In addition, the negative charge on the side chain of E111 is only 4–5 Å away from the side chain of T452. If K519 of ClC-0 corresponds to T452 of the bacterial ClC channels, it is

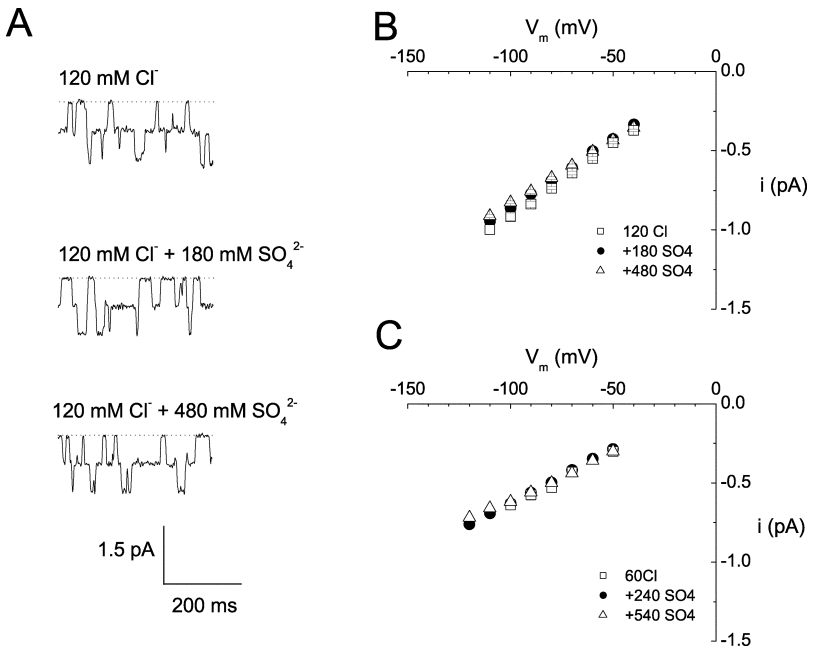

FIGURE 6. Absence of charge screening by a nonpermeant ion, SO_4^{2-}, on the conductance of the WT channel. (A) Single-channel recording traces of the WT channel at 120 mM symmetric $[Cl^-]$ with or without various concentrations of SO_4^{2-} (sodium salt) being added to the internal solution. (B) Single-channel i-V curves from recordings like those shown in A. $[Cl^-]_i$ = 120 mM. (C) Single-channel i-V curves from another set of experiments. $[Cl^-]_i$ = 60 mM.

likely that the negative charge from E127 would affect the functions of K519 in controlling the pore conductance. These structural observations suggest that E127 of ClC-0 may regulate the pore conductance if the Cl^- occupancy in the pore is affected by the side-chain charge of the pore residues.

To explore the functional role of E127 in ClC-0, we mutate this negatively charged residue into glutamine. Fig. 7 shows a comparison of the single-channel behaviors of the E127Q mutant with those of the WT channel. Surprisingly, the Cl^- dependence of the single-channel current (Fig. 7 A) and the fast-gate P_o-V curve (Fig. 7 B) of the E127Q mutant are nearly identical to those of the WT channel. However, although the E127Q mutation by itself appears to have little effect on the pore conductance of the WT channel, its functional role is revealed when double mutations at positions 127 and 519 are made. Fig. 8 A shows representative single-channel traces of various mutants at position 519 in the absence and in the presence of E127Q mutation. In the presence of glutamate at position 127 (E127), the charge at position 519 exerts an electrostatic influence on the pore conductance—the replacement of K519 with a neutral or a negatively charged residue decreases the single-channel current amplitude. In the background of E127Q mutation, however, the mutants with a positive and a neutral charge at position 519 appear to have similar channel conductance. With a negative charge at position 519, the current amplitudes of the double mutants (E127Q/K519E and E127Q/K519D) are not as small as those of the K519E and K519D single-point mutants. The averaged single-channel conductance of these double mutants at various $[Cl^-]_i$ are compared in Fig. 8 B. The fitted curves for the data obtained from the WT channel (K519) and those of the single-point mutants, K519C and K519E, are reproduced as dotted curves. In the presence of E127Q mutation, the channels with a neutral or a positively charged residue at position 519 (that is, E127Q/K519C and E127Q/K519) have a similar conductance-Cl^- activity curve as that of the WT channel. The curve for the E127Q/K519E double mutant, although significantly different, also approaches that of the WT channel. Like the single-point mutations at position 519, these Cl^- titration curves all have a similar maximal conductance at a saturated $[Cl^-]_i$ (see Table I), but the apparent affinities are changed by the mutations.

Although all the above mutations involving residues 127 and 519 appear to change only the apparent affinity of the conductance-Cl^- activity curve, the charge mutations at the inner pore mouth can also alter the maximal pore conductance (Fig. 9). This finding came from mutations in which a positively charged residue lysine was placed at positions 127 and 515. The E127K single-point mutant did not show functional current (more than five runs of channel expressions). However, the double mutant E127K/K519E did express. The position 515 is comparable to position 127 in that both are at an approximate equal distance from S_{cen} or from S_{int} (see Fig. 1). Fig. 9 A shows the single-channel recording traces of these two mutants in comparison with those of the WT and the K519E channels at two $[Cl^-]_i$. The Cl^- titration curves of the pore conductance are shown in Fig. 9 B. Both mutants have a comparable pore conductance throughout a wide range of $[Cl^-]_i$. At a low $[Cl^-]_i$, the conductance of these two mutants is

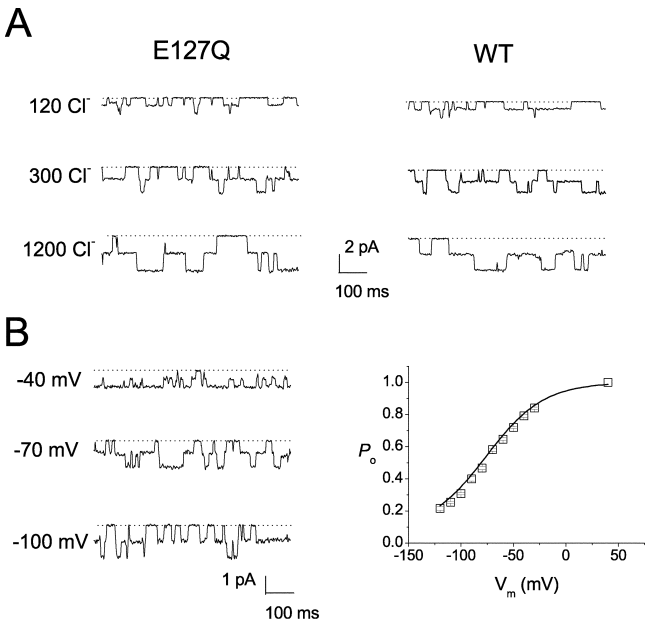

FIGURE 7. Gating and permeation properties of the E127Q mutant at the single-channel level. (A) Comparison of single-channel current between WT and the E127Q channels at various $[Cl^-]_i$. All recordings were with the excised inside-out configuration. The pipette solution contains 120 mM Cl^-, and the Cl^- concentrations at the intracellular side are indicated on the left. (B) Voltage-dependent gating of the E127Q mutant derived from single-channel recordings. (Left) Single-channel recordings from excised inside-out patches at three voltages. Symmetrical 120 mM $[Cl^-]$. (Right) Mean P_o-V curve of the E127Q mutant. Solid curve is the P_o-V curve of the WT channel.

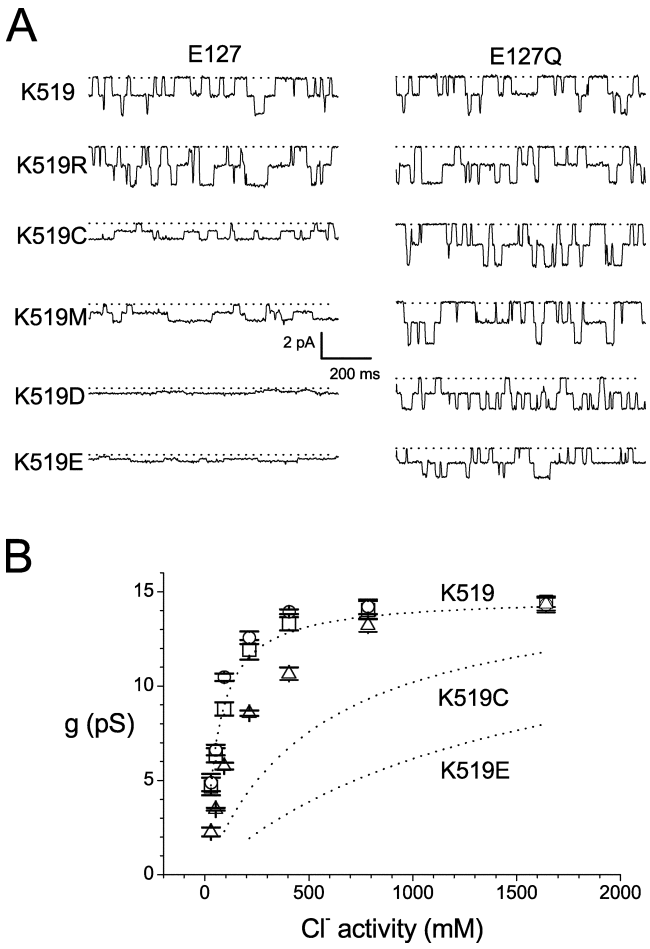

FIGURE 8. Comparison of the charge effects from position 519 on the single-channel current with or without E127Q mutation. (A) Single-channel recording traces of single (residue 519, left) and double mutants (residues 127 and 519, right) of ClC-0. All recordings were from the excised inside-out patch. $[Cl^-]_i$ and $[Cl^-]_o$ were 120 and 300 mM, respectively. $V_m = -110$ mV. (B) Conductance of double mutants at positions 127 and 519 as a function of internal Cl^- activity. Symbols are: squares, E127Q/K519; circles, E127Q/K519C; triangles, E127Q/K519E. Dotted curves are the same curves as those in Fig. 5 B. Curve fittings to Eq. 1b for the double mutants are not shown. The fitted values for g_{max} and $K_{1/2}$ are shown in Table I.

greater than that of the K519E mutant, consistent with the idea that more positive charge at the inner pore mouth helps Cl^- flow into the pore. However, at high $[Cl^-]_i$, the pore conductance saturates to ~8 pS—the charge mutations at the inner pore mouth can alter the maximal channel conductance. A positive charge in the pore probably results in a tight binding of Cl^-, thus reducing the throughput rate of Cl^- across the channel pore. Because the internal Cl^--binding site (S_{int}, in Dutzler et al., 2003) is closer to residues E127 and I515 than the binding site at S_{cen}, the charge effects from positions K519, E127, and I515 may come from altering the Cl^- binding to this internal binding site (see DISCUSSION).

Mutations at the Cl^- Selectivity Filter Mainly Affect the Saturated Pore Conductance

The crystal structures of the bacterial ClC channels revealed the amino acid residues that coordinate the bound Cl^- at the selectivity filter (Dutzler et al., 2002, 2003). We thus also explored the functional roles of the Cl^- selectivity filter in the ion permeation process. To this end, the Cl^- titration curves of the conductance of two mutants at the selectivity filter, S123T and Y512F, were examined. The positions of these two residues correspond to those of S107 and Y445 of the bacterial ClC channels (see Fig. 1 for their positions), and the oxygen atom of the side-chain hydroxyl group of these two residues coordinates the bound Cl^- ion (Dutzler et al., 2002). These mutations are thus likely to alter the binding energy of Cl^- at the selectivity filter. In the literature, the S123T mutant has been known to have a small channel conductance—at physiological Cl^- concentrations, this mutant channel has a conductance of ~2 pS, a value very similar to that of the K519E mutant

TABLE I

Maximal Pore Conductance (g_{max}) and Half Saturated Internal Cl^- Activities ($K_{1/2}$) of the WT Channel and Various Mutants

Channels	g_{max}	$K_{1/2}$
	pS	*mM*
K519	14.7 ± 0.3	58.9 ± 4.8
K519R	14.8 ± 0.4	80.7 ± 11.4
K519C	15.7 ± 0.6	533.9 ± 46.0
K519M	15 ± 0*	564.3 ± 49.4
K519D	15 ± 0*	2,044.4 ± 323.1
K519E	15 ± 0*	1,444.3 ± 276.0
E127Q/K519	15.3 ± 0.2	67.0 ± 3.5
E127Q/K519R	13.8 ± 0.4	36.6 ± 6.7
E127Q/K519C	15.4 ± 0.5	55.2 ± 7.4
E127Q/K519H	15.7 ± 0.2	51.2 ± 3.0
E127Q/K519M	16.8 ± 0.6	70.7 ± 10.1
E127Q/K519D	16.4 ± 0.5	152.6 ± 15.4
E127Q/K519E	15.9 ± 0.3	177.8 ± 10.8
S123T	2.6 ± 0.2	69.1 ± 21.5
Y512F	20.9 ± 0.5	87.4 ± 7.4

This table reports the parameters g_{max} and $K_{1/2}$ derived by fitting the conductance-Cl^- activity curves of various channels to a Michaelis-Menten type equation (Eq. 1b). In most cases, g_{max} and $K_{1/2}$ were free parameters. For the g_{max} values indicated by *, the number of points were not enough to give a reasonable fit to the Michaelis-Menten curve. Therefore, the value 15 pS was assigned to evaluate the other parameter $K_{1/2}$.

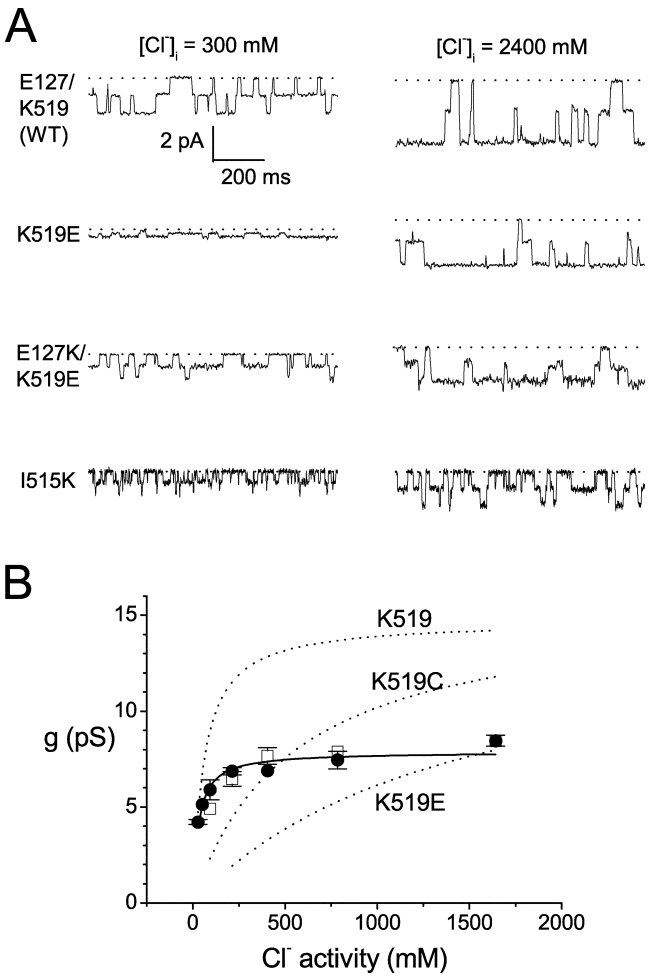

FIGURE 9. Effects of a positive charge at position 127 and 515 on the single-channel conductance of ClC-0. (A) Representative single-channel traces for WT (E127/K519), the single-point mutant K519E, I515K and the double mutant E127K/K519E. V_m = −110 mV; $[Cl^-]_o$ = 120 mM; $[Cl^-]_i$ are as indicated. (B) Comparison of the conductance-Cl^- activity curves of E127K/K519E (filled circles) and I515K (open squares) with those of the WT, K519C, and K519E channels (dotted curves). Solid curve is the best fit of the data points from E127K/K519E double mutant to Eq. 1b. The fitted g_{max} and $K_{1/2}$ are 8.5 pS and 27.5 mM, respectively.

(Ludewig et al., 1996). In Fig. 10 A, we compare the single-channel traces of S123T and Y512F mutants with those of the WT channel (K519) and the K519E mutant. The $[Cl^-]_i$ titration curves of the channel conductance are shown in Fig. 10 B. At a low $[Cl^-]_i$, for example 300 mM, the conductance of S123T is 2 pS, a value similar to that of the K519E mutant. At a high $[Cl^-]_i$, however, the conductance of S123T remains small (2.5 pS at 2,400 mM), whereas that of the K519E mutant is increased to 9 pS at the same $[Cl^-]_i$. These results thus indicate that the cause of reduced conductance by K519E and S123T mutations is different in each case because the small conductance of K519E can be increased by high $[Cl^-]_i$, while the conductance of S123T remains small at saturated $[Cl^-]_i$. For the Y512F mutant, the channel conductance is already larger than that of the WT channel at low $[Cl^-]_i$. When $[Cl^-]_i$ is increased, its value saturates to ~21 pS, ~30% higher than that of the WT channel. However, the change in the apparent Cl^- affinity in this mutant is very small in comparison to those of the K519C and K519E mutants. These results thus suggest that the regulations of channel conductance by mutations at the selectivity filter and at the inner pore mouth are different. The charges of E127 and K519 might determine the occupancy of Cl^- at the internal Cl^--binding site. On the other hand, the mutations S123T and Y512F probably change the Cl^- exit rate from the selectivity filter, thus altering the saturated Cl^- conductance.

DISCUSSION

Regulation of pore conductance by fixed charges near the pore region has been shown in many ion channels. Altering the charge of the lipid used in the bilayer recording experiments can change the conductance of the channels (Bell and Miller, 1984). The manipulations of the fixed charge on the channel protein by chemical modifications or site-directed mutagenesis also affect the ion permeation (Imoto et al., 1986, 1988; MacKinnon and Miller 1989; MacKinnon et al., 1989;

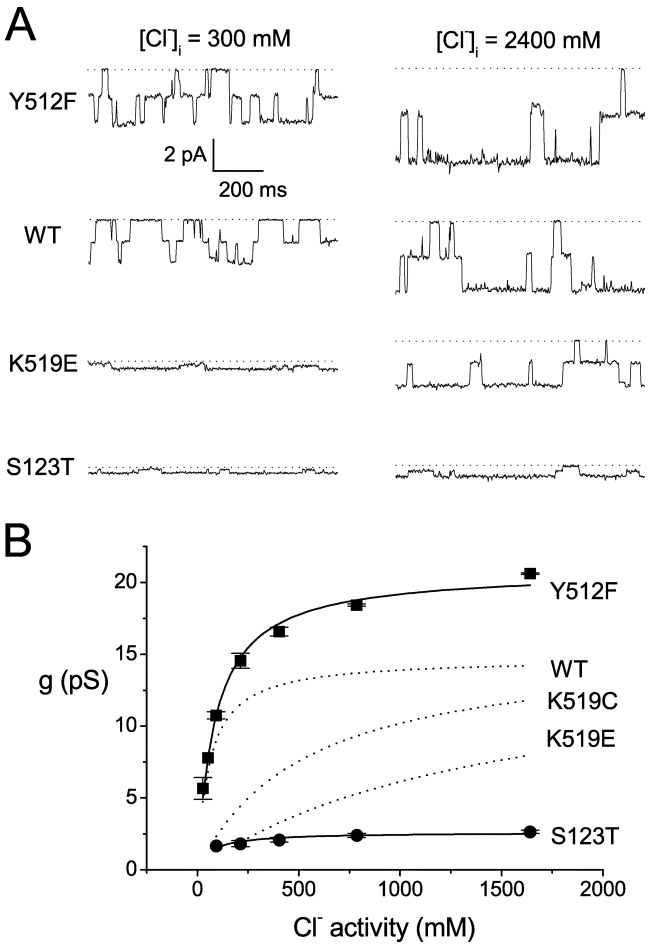

FIGURE 10. Conductance determinants along the pore of ClC-0. (A) Single-channel recording traces of the S123T and Y512F mutants at two $[Cl^-]_i$. For comparisons, the traces for the WT and K519E channels are also shown. All recording traces were taken at −110 mV. $[Cl^-]_o$ = 120 mM. (B) Conductance-Cl^- activity curves of the S123T and Y512F mutants. Data points were fitted to Eq. 1b, with g_{max} and $K_{1/2}$ values shown in Table I. Dotted curves are those of WT, K519C, and K519E channels.

Pappone and Barchfeld, 1990; Kienker et al., 1994; Middleton et al., 1996). In most cases, a fixed negative charge increased the cation conductance, whereas a positive charge increased the anion conductance. In the extreme examples, the ion selectivity of a channel can be reversed from cationic to anionic, or vice versa, with mutations of a limited number of key residues (Galzi et al., 1992; Keramidas et al., 2000). In all these preceding examples, the underlying mechanism can be a simple surface charge mechanism or a more complicated regulation of the occupancy of permeant ions in the pore. In ClC-0, the conductance regulations by charged residues at the inner pore mouth are more consistent with the latter mechanism, because the effect cannot be screened out by high concentrations of nonpermeant ions (Fig. 6).

The mechanisms for controlling the conductance of ion channels ultimately come from the interaction between the permeant ion and the pore-lining amino acid residues. The pore allows the permeation of ions with a diameter smaller than that of the pore, and thus serves as a molecular sieve. The electrostatic force or the dipole arrangement from the protein molecule can help stabilize the charged ion in the middle of the lipid bilayer (Doyle et al., 1998; Dutzler et al., 2002, 2003). In ClC channels, the Cl^- permeation mechanism is not as well understood as those in the voltage-gated cation channels. Although mutations of several amino acid residues were shown to alter the permeability ratios or to change the single-channel current amplitude in a variety of ClC channels (Ludewig et al., 1996, 1997; Fahlke et al., 1997; Lin and Chen, 2000), the underlying mechanisms of these mutational effects were unclear. The present study for the first time reveals functionally that there are separate determinants in the ion permeation pathway of ClC-0 that can control the pore conductance. This conclusion is best illustrated by the effects of raising $[Cl^-]_i$ on the conductance of K519E and S123T mutants. Although these two mutations reduce the WT channel conductance to a similar level at physiological Cl^- concentrations, the underlying mechanisms for the decrease in conductance in these two mutants are different because an elevation of $[Cl^-]_i$ can increase the conductance of the mutant K519E but not that of S123T. The observation that most of the mutations at the inner pore mouth affect the apparent $K_{1/2}$ of the conductance concentration curve, while those mutations at the selectivity filter alter the maximal channel conductance, also suggests at least two different conductance determinants in the ClC-0 pore.

The meaning of the separate conductance determinants is revealed from the most recent crystal structure of the *E. coli* ClC channel solved to 2.5-Å resolution (Dutzler et al., 2003), in which multiple Cl^--binding sites in the pore were identified . We adopt this new structural model for ClC channels, and propose that the above separate conductance determinants may represent two ion-binding sites in the pore of ClC-0. In its simplest form, a single-ion occupied pore, the two-site model is represented by the following scheme:

$$Ch + Cl_{in} \underset{k_{-1}}{\overset{k_1}{\rightleftharpoons}} Ch \bullet Cl \xrightarrow{k_2} Ch^* \bullet Cl \xrightarrow{k_3} Ch + Cl_{out}$$

where Ch, Cl_{in}, and Cl_{out} represent channel pore, internal Cl^-, and external Cl^-, respectively. The model distinguishes two ion binding sites represented by Ch•Cl and Ch*•Cl. The constants, k_1, k_{-1}, k_2, and k_3 are microscopic rates associated with each kinetic step. Since our recordings examine the outward Cl^- movement (inward current), the ion permeation process is initiated by the binding of an internal Cl^- (Cl_{in}) to the in-

ternal site Ch•Cl followed by the movement of the Cl^- from this internal site to Ch*•Cl, and finally the exiting of the bound Cl^- from Ch*•Cl to external solution (Cl_{out}). This two-site model thus predicts that at a steady-state the current (i) and the derived pore conductance (g) are related to the internal Cl^- activity (A_{Cl}) with a Michaelis-Menten equation:

$$i = i_{max} \times A_{Cl}/(A_{Cl} + K_{1/2}), \quad (1a)$$

$$g = g_{max} \times A_{Cl}/(A_{Cl} + K_{1/2}), \quad (1b)$$

where

$$i_{max} = [(k_2 \times k_3)/(k_2 + k_3)] \times 1.6 \times 10^{-19}, \quad (2)$$

and

$$K_{1/2} = [k_3/(k_2 + k_3)] \times (k_{-1}/k_1). \quad (3)$$

We assume that the leaving of the bound Cl^- from the site represented by Ch*•Cl is the rate-limiting step of the entire ion permeation process in the saturated Cl^- concentration. On the other hand, since g_{max} as well as $K_{1/2}$ can be altered by the charge mutations surrounding the site Ch•Cl, we suggest k_1, k_{-1}, or k_2 can be changed by these mutations. Consequently, mutations that affect the binding of Cl^- to the internal site could either change the Cl^- apparent affinity, the saturated pore conductance, or both. Without multiple ion-binding sites in the pore, it is difficult to explain all the results in this study. In a single-site model, for example, it would be impossible to alter the rate-limiting step without significantly changing the apparent Cl^- affinity. Thus, the functional data support the presence of multiple Cl^--binding sites in the pore of ClC-0.

By comparing the functional results from ClC-0 with the crystal structure of bacterial ClC channels, it is tempting to suggest that the sites represented by Ch•Cl and Ch*•Cl in the above functional model could correspond, respectively, to the S_{int} and S_{cen} sites in the bacterial ClC channels. If this is the case, the negative charge of E127 is ~6–7 Å away from S_{int}, and should influence the Cl^- binding to this internal site. However, its negativity is likely to be reduced by the positive charge from K519 because the side chains of these residues are only 4–5 Å apart. One can imagine that when the positive charge from K519 is removed, the electrostatic field surrounding E127 may become more negative, and this could reduce k_1 and/or increase k_{-1} and k_2. However, the maximal channel conductance is still controlled by k_3 because it is the rate-limiting step. When a positive charge is placed at position 127 or 515 (such as E127K and I515K), the binding of Cl^- at S_{int} is very tight. This may reduce the rate of k_2 significantly to a value that is comparable to, or even smaller than, k_3, and therefore the saturated conductance of these mutants is reduced. When the mutations at the selectivity filter (such as S123T and Y512F) are made, the most prominent change is on the saturated channel conductance because the rate-limiting step of ion permeation is altered.

The unequal contribution of the side-chain charge from residue E127 and K519 is also plausible because the former is closer to the position of S_{int}. Thus, E127 plays a more critical role in affecting channel conductance. Although the charges from these two residues most likely combine to control the Cl^- occupancy at the site of S_{int}, their functional roles may not be the same. We envision a "pull and push" mechanism, in which the positive charge of K519 contributes more to pull Cl^- into the pore while the negative charge on E127 is more important to repel Cl^- so that the translocation of Cl^- from S_{int} to S_{cen} proceeds more easily. Such an arrangement may solve the paradox created by the presence of charged residues in the ion permeation pathway. The unequal electrostatic contributions from E127 and K519, however, are less prominent in selecting charged MTS compounds applied to the intracellular side of these two residues (Lin and Chen, 2003).

Thus, the implication of the functional results obtained in ClC-0 is surprisingly consistent with the structure of the bacterial ClC channel, even though the *Torpedo* channel and the bacterial channel share only ~20% overall sequence identity. The conductance determinants presented in this study may correspond to the ion-binding sites S_{int} and S_{cen} in the bacterial ClC channel pore (Dutzler et al., 2003). Is there a third Cl^--binding site like the S_{ext} site of the bacterial ClC channel? This external binding site is positioned at the location of the negative charge of E148 in the bacterial ClC channel, which corresponds to E166 of ClC-0. The negatively charged side chain of this glutamate occludes the channel pore, and thus could serve as the gate for the channel (Dutzler et al., 2002). It was demonstrated that a permeant ion is located at this position when this negatively charged side chain is removed by mutagenesis (Dutzler et al., 2003). The present study does not provide evidence that specifically address the functional role of S_{ext} in ClC-0 pore conductance. We speculate, however, that if this external Cl^--binding site exists in ClC-0 pore, it may have a lower intrinsic Cl^--binding affinity than that of the S_{cen} site because Cl^- needs to compete with the negative charge on the E166 side-chain for this site. Such a three-binding-site model with a rate-limiting step at the selectivity filter would still generate similar overall behaviors in the ion flux across the pore as discussed above.

The above discussions and Eqs. 1–3 are all based on the one-ion occupancy model because the single-chan-

nel conductance-Cl^- activity curve appears to be a simple saturation curve as if there is only one ion in the pore (Andersen, 1989). Previous functional studies of the ClC-0 conductance at the single-channel level also came to the same conclusion—the ion conduction process of ClC-0 is consistent with a single-ion Eyring model in which the ion traverses multiple kinetic barriers as it permeates the pore (White and Miller, 1981). As crystal structures of the bacterial channel reveal three ions bound in the pore of the bacterial ClC channels, it is unclear if this is a true difference between *Torpedo* and bacterial channels. But more likely, the apparent properties of one-ion occupancy in ClC-0 may result from inadequate functional studies in this *Torpedo* channel so that the multiple-ion nature of the pore is not revealed. Thus, the model presented above should be considered as only tentative. It would await more precise functional measurements and direct structural studies of ClC-0 to fully address its ion permeation mechanism.

Finally, the possible competition of the Cl^- occupancy with the negatively charged E166 side chain at the site S_{ext} is interesting since this might be responsible for the "gating-permeation coupling" in ClC-0 (Pusch et al., 1995; Chen and Miller, 1996). Because of the intimate relation of the ClC-0 gating with permeant ions, mutations that affect Cl^- permeation are likely to alter the channel gating as well. Indeed, by examining the single-channel recording traces of the mutants presented in this work, it is apparent that the fast gating of the channel is also changed. For example, at the same $[Cl^-]_i$, the average duration of the open events of the K519E and K519C appears to be longer than that of the WT channel (Fig. 4). At the same time, increasing $[Cl^-]_i$ also prolongs the duration of the open events (Fig. 4). We are in the process of analyzing the fast-gating parameters in these mutants to explore the Cl^- regulation and the side-chain charge effects on the fast gating of ClC-0.

We thank Dr. R. Fairclough and Dr. T.-C. Hwang for their insightful discussions of the work, and the critical readings of the manuscript. We are also grateful to Dr. R. MacKinnon for kindly revealing to us the 2.5-Å bacterial ClC channel structure prior to its publication.

This work was partly supported by a Health Science Research Award from University of California-Davis School of Medicine and a National Institutes of Health grant GM-65447.

Olaf S. Andersen served as editor.

Submitted: 7 April 2003
Accepted: 7 July 2003

REFERENCES

Andersen, O.S. 1989. Kinetics of ion movement mediated by carriers and channels. *Methods Enzymol.* 171:62–112.

Bauer, C.K., K. Steinmeyer, J.R. Schwarz, and T.J. Jentsch. 1991. Completely functional double-barreled chloride channel expressed from a single *Torpedo* cDNA. *Proc. Natl. Acad. Sci. USA.* 88: 11052–11056.

Bell, J., and C. Miller. 1984. Effects of phospholipid surface charge on ion conduction in the K^+ channel of sarcoplasmic reticulum. *Biophys. J.* 45:279–287.

Chen, M.-F., and T.-Y. Chen. 2001. Different fast-gate regulation by external Cl^- and H^+ of the muscle-type ClC chloride channel. *J. Gen. Physiol.* 118:23–32.

Chen, T.-Y. 1998. Extracellular zinc ion inhibits ClC-0 chloride channels by facilitating slow gating. *J. Gen. Physiol.* 112:715–726.

Chen, T.-Y., and C. Miller. 1996. Nonequilibrium gating and voltage dependence of the ClC-0 Cl^- channel. *J. Gen. Physiol.* 108:237–250.

Doyle, D.A., J.H. Morais-Cabral, R.A. Pfuetzner, A. Kuo, J.M. Gulbis, S.L. Cohen, B.T. Chait, and R. MacKinnon. 1998. The structure of the potassium channel: Molecular basis of K^+ conduction and selectivity. *Science.* 280:69–77.

Dutzler, R., E.B. Campbell, M. Cadene, B.T. Chait, and R. MacKinnon. 2002. X-ray structure of a ClC chloride channel at 3.0 Å reveals the molecular basis of anion selectivity. *Nature.* 415:287–294.

Dutzler, R., E.B. Campbell, and R. MacKinnon. 2003. Gating the selectivity filter in ClC chloride channels. *Science.* 300:108–112.

Fahlke, C., H.T. Yu, C.L. Beck, T.H. Rhodes, and A.L. George, Jr. 1997. Pore-forming segments in voltage-gated chloride channels. *Nature.* 390:529–532.

Galzi, J.-L., A. Devillers-Thiéry, N. Hussy, S. Bertrand, J.-P. Changeux, and D. Bertrand. 1992. Mutations in the channel domain of a neuronal nicotinic receptor convert ion selectivity from cationic to anionic. *Nature.* 359:500–505.

Green, W.N., and O.S. Andersen. 1991. Surface charges and ion channel functions. *Annu. Rev. Physiol.* 53:341–359.

Hanke, W., and C. Miller. 1983. Single chloride channels from *Torpedo* electroplax: activation by protons. *J. Gen. Physiol.* 82:25–45.

Hamill, O.P., A. Marty, E. Neher, B. Sakmann, and F.J. Sigworth. 1981. Improved patch-clamp techniques for high-resolution current recording from cells and cell-free membrane patches. *Pflugers Arch.* 391:85–100.

Hille, B. 2001. Elementary properties of ions in solution. *In* Ion Channel of Excitable Membrane. 3rd ed. B. Hille, editor. Sinauer Associates, Inc., Sunderland, MA. 309–345.

Imoto, K., C. Busch, B. Sakmann, M. Mishina, T. Konno, J. Nakai, H. Bujo, Y. Mori, K. Fukuda, and S. Numa. 1988. Rings of negatively charged amino acids determine the acetylcholine receptor channel conductance. *Nature.* 335:645–648.

Imoto, K., C. Methfessel, B. Sakmann, M. Mishina, Y. Mori, T. Konno, K. Fukuda, M. Kurasaki, H. Bujo, Y. Fujita, and S. Numa. 1986. Location of a δ-subunit region determining ion transport through the acetylcholine receptor channel. *Nature.* 324:670–674.

Iyer, R., T.M. Iverson, A. Accardi, and C. Miller. 2002. A biological role for prokaryotic ClC chloride channels. *Nature.* 419:715–718.

Jentsch, T.J., T. Friedrich, A. Schriever, and H. Yamada. 1999. The CLC chloride channel family. *Pflügers Arch.-Eur. J. Physiol.* 437: 783–795.

Jentsch, T.J., V. Stein, F. Weinreich, and A. Zdebik. 2002. Molecular structure and physiological function of chloride channels. *Physiol. Rev.* 82:503–568.

Jentsch, T.J., K. Steinmeyer, and G. Schwarz. 1990. Primary structure of *Torpedo marmorata* chloride channel isolated by expression cloning in *Xenopus* oocytes. *Nature.* 348:510–514.

Keramidas, A., A.J. Moorhouse, C.R., French, P.R. Schofield, and P.H. Barry. 2000. M2 pore mutations convert the glycine receptor channel from being anion- to cation-selective. *Biophys. J.* 78:247–259.

Kienker, P., G. Tomaselli, M. Jurman, and G. Yellen. 1994. Conductance mutations of the nicotinic acetylcholine receptor do not act by a simple electrostatic mechanism. *Biophys. J.* 66:325–334.

Lin, C.-W., and T.-Y. Chen. 2000. Cysteine modification of a putative pore residue in ClC-0: implication for the pore stoichiometry of ClC chloride channels. *J. Gen. Physiol.* 116:535–546.

Lin, C.-W., and T.-Y. Chen. 2003. Probing the pore of ClC-0 by substituted cysteine accessibility method using methane thiosulfonate reagents. *J. Gen. Physiol.* 122:225–237.

Lin, Y.-W., C.-W. Lin, and T.-Y Chen. 1999. Elimination of the slow gating of ClC-0 chloride channel by a point mutation. *J. Gen. Physiol.* 114:1–12.

Ludewig, U., T.J. Jentsch, and M. Pusch. 1997. Analysis of a protein region involved in permeation and gating of the voltage-gated *Torpedo* chloride channel ClC-0. *J. Physiol.* 498:691–702.

Ludewig, U., M. Pusch, and T.J. Jentsch. 1996. Two physically distinct pores in the dimeric ClC-0 chloride channel. *Nature.* 383: 340–343.

MacKinnon, R., and C. Miller. 1989. Functional modification of a Ca^{2+}-activated K^+ channel by trimethyloxonium. *Biochemistry.* 28: 8087–8092.

MacKinnon, R., R. Latorre, and C. Miller. 1989. Role of surface electrostatics in the operation of a high-conductance Ca^{2+}-activated K^+ channel. *Biochemistry.* 28:8092–8099.

Maduke, M., C. Miller, and J.A. Mindell. 2000. A decade of CLC chloride channels: structure, mechanism, and many unsettled questions. *Annu. Rev. Biophys. Biomol. Struct.* 29:411–438.

Middleton, R.E., D.J. Pheasant, and C. Miller. 1994. Purification, reconstitution, and subunit composition of a voltage-gated chloride channel from *Torpedo* electroplax. *Biochemistry.* 33:13189–13198.

Middleton, R.E., D.J. Pheasant, and C. Miller. 1996. Homodimeric architecture of a ClC-type chloride ion channel. *Nature.* 383:337–340.

Miller, C. 1982. Open-state substructure of single chloride channels from *Torpedo* electroplax. *Phil. Trans. R. Soc. Lond. B Biol. Sci.* 299: 401–411.

Miller, C., and E.A. Richard. 1990. The *Torpedo* chloride channel: intimations of molecular structure from quirks of single-channel function. *In* Chloride Transporters. A. Leefmans and J. Russel, editors. Plenum Press, New York. 383–405.

Miller, C., and M.M. White. 1984. Dimeric structure of single chloride channels from *Torpedo* electroplax. *Proc. Natl. Acad. Sci. USA.* 81:2772–2775.

O'Neill, G.P., R. Grygorczyk, M. Adam, and A.W. Ford-Hutchinson. 1991. The nucleotide sequence of a voltage-gated chloride channel from the electric organ of *Torpedo californica. Biochim. Biophys. Acta.* 1129:131–134.

Pappone, P.A., and G.L. Barchfeld. 1990. Modifications of single acetylcholine-activated channels in BC3H-1 cells. *J. Gen. Physiol.* 96:1–22.

Pusch, M., A. Accardi, A. Liantonio, L. Ferrera, A. De Luca, D.C. Camerino, and F. Conti. 2001. Mechanism of block of single protopores of the *Torpedo* chloride channel ClC-0 by 2-(*p*-chlorophenoxy)butyric acid (CPB). *J. Gen. Physiol.* 118:45–62.

Pusch, M., U. Ludewig, A. Rehfeldt, and T.J. Jentsch. 1995. Gating of the voltage-dependent chloride channel ClC-0 by the permeant anion. *Nature.* 373:527–531.

Robinson, R.A., and R.H. Stokes. 1955. Activity coefficients of electrolytes at 25°C. *In* Electrolyte Solutions. Academic Press Inc., New York, NY. 477 pp.

White, M.M., and C. Miller. 1981. Probes of the conductance process of a voltage-gated Cl^- channel from *Torpedo* Electroplax. *J. Gen. Physiol.* 78:1–18.